Research Article

Sikander Ali*, Ghanwa Tahir, Muhammad Usman Ahmad, Iram Liaqat, Muhammad Nauman Aftab, Shazia Khurshid, Jahangir Khan, Abid Sarwar, Tariq Aziz*, Metab Alharbi, Abdullah F. Alasmari, and Thamer H. Albekairi

Green synthesis and effective utilization of biogenic Al_2O_3-nanocoupled fungal lipase in the resolution of active homochiral 2-octanol and its immobilization via aluminium oxide nanoparticles

https://doi.org/10.1515/gps-2024-0141
received June 14, 2024; accepted October 08, 2024

Abstract: The present study highlights the true potential of *Rhizopus oligosporus* IIB-08 to produce lipase enzyme under solid-state fermentation and focuses on improving the properties of lipase by immobilizing it on biogenic aluminium oxide nanoparticles (Al-NPs) for better resolution of active homochiral 2-octanol. For this purpose, almond meal substrate showed 10.44 ± 0.36 $U{\cdot}g^{-1}$ lipase activity. The immobilization of lipase on biogenic Al-NPs prepared using *Mentha spicata* leaf extract led towards improved stability and catalytic efficiency, resulting in a 9.3% increase in activity compared to free enzyme. This study also examined the potential of the immobilized lipase in the effective resolution of 2-octanol. Gas chromatography-mass spectrometry confirmed the presence of lipase-catalysed fatty acids, such as linolenic acid (C18:3), linoleic acid (C18:2), palmitic acid, and oleic acid (C18:1), with palmitic acid exhibiting the highest concentration (142 $\mu g{\cdot}ml^{-1}$) at a retention time of 23.2 min. This study concludes that *R. oligosporus* IIB-08 is a promising source for lipase production and demonstrates the significant potential of nanoparticle-immobilized lipase in resolving pharmaceutically important organic chemicals, thereby making it a promising approach for different industrial applications. However, further scaling up is needed for better implementation in the industry.

Keywords: lipase, immobilization, biosynthesis, *Mentha spicata*, aluminium oxide nanoparticles, 2-octanol

*** Corresponding author: Sikander Ali**, Department of Microbiology, Dr. Ikram-ul-Haq Institute of Industrial Biotechnology, Government College University Lahore, Lahore, Pakistan, e-mail: dr.sikanderali@gcu.edu.pk
*** Corresponding author: Tariq Aziz**, Laboratory of Animal Health, Food Hygiene and Quality, Department of Agriculture, University of Ioannina, 47100, Arta, Greece; Institute of Molecular Biology and Biotechnology, The University of Lahore, Punjab, Pakistan, e-mail: iwockd@gmail.com
Ghanwa Tahir, Muhammad Usman Ahmad: Department of Microbiology, Dr. Ikram-ul-Haq Institute of Industrial Biotechnology, Government College University Lahore, Lahore, Pakistan
Iram Liaqat: Department of Zoology, Science Block, GCU Lahore, Lahore, Pakistan
Muhammad Nauman Aftab: Department of Biotechnology, Dr. Ikram-ul-Haq Institute of Industrial Biotechnology, Government College University Lahore, Lahore, Pakistan
Shazia Khurshid, Jahangir Khan: Department of Chemistry, Institute of Chemical Sciences, Government College University Lahore, Lahore, Pakistan
Abid Sarwar: Food and Biotechnology Research Centre, Pakistan Council of Scientific Industrial Research (PCSIR), Lahore, 54600, Pakistan.
Metab Alharbi, Abdullah F. Alasmari, Thamer H. Albekairi: Department of Pharmacology and Toxicology, College of Pharmacy, King Saud University, P.O. Box 2455, Riyadh, 11451, Saudi Arabia

1 Introduction

Lipases (EC 3.1.1.3) are classified in the hydrolases family and belong to the class of serine hydrolases. These remarkable enzymes can hydrolyze carboxyl ester groups present in long-chain acylglycerols (>10 C atoms), as shown in Figure 1a. These enzymes naturally catalyse various reactions, such as the hydrolysis of triglycerides [1,2]. The industrial importance of lipases is owing to their selectivity and exceptional catalytic efficiency, making them extensively applicable in several industries such as animal feed, amino acid derivatives, food, pharmaceutical, dairy, biofuel, cleaning, flavour, perfumery, esters, agrochemicals, bioremediation, cosmetics, and biosensors [3].

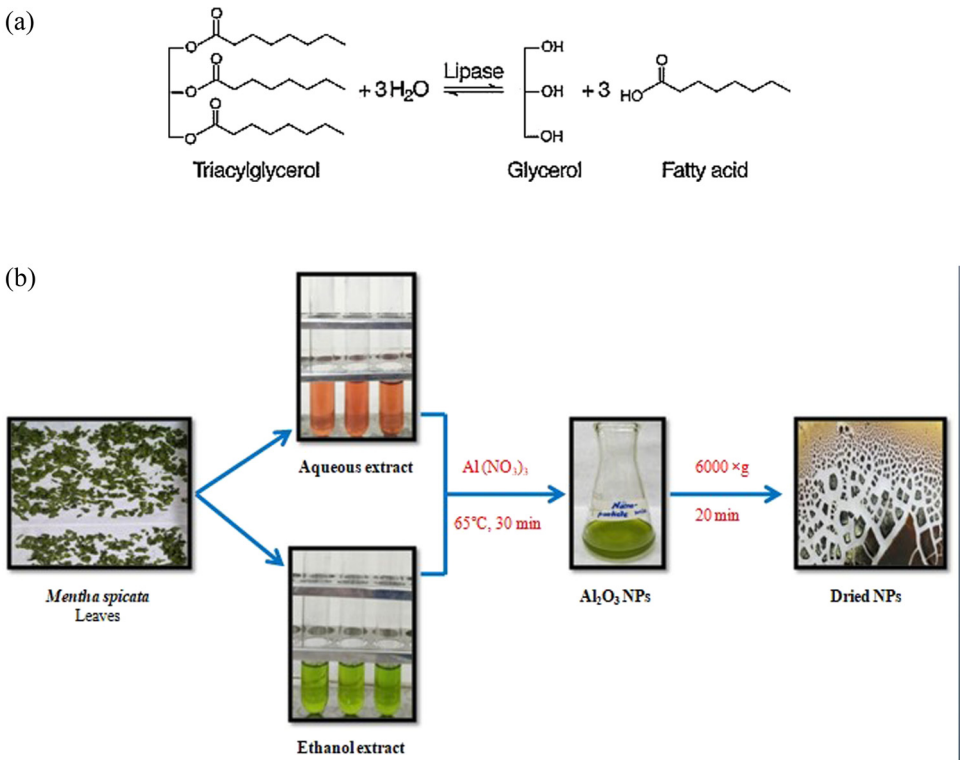

Figure 1: (a) Lipase enzyme-catalysed hydrolysis process. (b) Al-NP synthesis using *M. spicata* leaf extract.

A vast plethora of sources are available for the production of lipases; however, micoorganisms are reported as the best producers of lipases because of their high production and capability of carrying out various catalytic reactions [4]. Notably, the increased amounts of lipase production are well reported by some bacterial and fungal species such as *Pseudomonas* sp., *Streptomyces* sp., *Bacillus* sp., *Mucor* sp., *Aspergillus* sp., *Rhizomucor* sp., *Penicillium* sp., *Rhizopus* sp., and *Geotrichum* sp. [5]. The high diversity of substrate specificity and physical properties of microbial lipases necessitate the screening of the most suitable enzyme production systems [6]. Among various fermentation processes, solid-state fermentation (SSF) is an outstanding process to produce valuable products from low-cost agro-industrial wastes, which serve as essential nutrient sources in the fermentation process [7,8]. Various substrates, such as soybean meal, rice husk, and wheat straw, are used for the production of lipases; however, almond meal is the most suitable substrate as it contains basic nutritional components, which may increase the specific activity of different microbial lipases. As the commercial production cost of free lipases is very high, developing a cost-effective and stable immobilized lipase system is very crucial. Among the numerous matrices available, nanoparticles (NPs) offer many unique physicochemical properties for the cost-effective production of immobilized lipase [9].

Conventionally, different chemical methods are utilized for the synthesis of NPs; however, these methods often involve the use of some toxic chemicals that render the NPs unsuitable for biological applications [10]. Therefore, green nanotechnology has emerged as an alternative for the fabrication of biogenic NPs. Green synthesis of NPs not only avoids toxic chemicals but also clearly aligns with sustainable and eco-friendly approaches. Among various biogenic NPs, aluminium oxide nanoparticles (Al-NPs) from natural extracts have gained importance as an immobilization matrix [11]. In this study, *Mentha spicata* leaf extract was used for the synthesis of Al_2O_3 NPs due to its rich active phytochemical content, which includes flavonoids, polyphenols, and terpenoids, which serve as stabilizing and reducing agents, ensuring the effective fabrication of NPs. Additionally, *M. spicata* is easily available and has been documented to have excellent antioxidant properties, making it a suitable candidate for the green synthesis of NPs [12]. The presence of these phytochemicals facilitates the reduction of metal ions to Al-NPs by electron donation, thus leading to the formation of stable NPs. The NPs formed are highly favourable for better industrial applications of immobilized lipases.

Immobilized lipases catalyse reactions involving water-immiscible substances through hydrolysis processes, enabling the synthesis of optically active materials and functional compounds. One such compound is 2-octanol, an

organic homochiral compound synthesized through lipase-catalysed trans-esterification reaction [13,14]. Lipase-mediated resolution of 2-octanol offers significant benefits because it allows for the synthesis of compounds with high enantiomeric purity, which are important in the development of fine chemicals, pharmaceuticals, and agrochemicals. Furthermore, lipase-catalysed resolution of 2-octanol provides a more eco-friendly alternative to conventional chemical methods, which frequently require harsh chemicals and generate substantial waste. Utilizing immobilized lipase further enhances the process efficiency by allowing for the enzyme reuse and improving stability. The use of lipase for the resolution of 2-octanol has not been explored thoroughly, especially in Pakistani industries, despite its promising potential [15]. This study aims to address the existing research gap by showcasing the practicality and advantages of employing immobilized lipase for 2-octanol resolution, thereby effectively contributing to the advancement of sustainable and effective biocatalytic processes.

2 Materials and methods

The chemicals used during this work were of high-grade purity and procured from E-Merck (Germany) and Sigma Aldrich (USA). These chemicals include dioctyl sulfosuccinate sodium salt, gum acacia, *n*-hexane, acetyl chloride, 2-octanol, and aluminium nitrate nona-hydrate.

2.1 Organism and culture maintenance

A wild-type strain of *Rhizopus oligosporus* (IIB-08) was obtained from the Microbial Culture Bank, Institute of Industrial Biotechnology (IIB), GC University, Lahore. The organism was maintained on PDA slopes and stored at 4°C in a cold cabinet (MPR 1410, SANYO, Japan).

2.2 Production of lipase by *R. oligosporus*

Almond meal (dried at 70°C for 2 h) was used as a substrate for lipase production by SSF. Ten grams of almond meal and 10 ml distilled water were added (in a ratio of 1:1) to a 250 ml cotton-plugged flask and sterilized. The sterilized Monoxal O.T. (0.05%, w/v) solution was used for the preparation of homogeneous conidial suspension. The flask was inoculated using 1 ml of inoculum aseptically and incubated in an Eco Cell static incubator at 30°C for 72 h [16]. All the batch culture experiments were conducted in a set of three parallel replicates.

2.3 Analytical techniques

2.3.1 Enzyme extraction

After the fermentation process was completed, 100 ml of distilled water was added to the flask and incubated in a shaking incubator (IrmecoGmBH, Germany) at 160 rpm and 30°C for 1 h. The contents of the flask were filtered, and the substrate free enzyme extract was used for the determination of lipase activity.

2.3.2 Determination of lipase activity

The enzyme activity in the fermented almond meal was determined titrimetrically based on the hydrolysis of olive oil. The supernatant of the fermented sample (1 ml) was added to the reaction mixture containing 1% olive oil in 1% gum acacia (10 ml), 5 ml phosphate buffer of pH 7.0, and 0.6% $CaCl_2$ (2 ml). The flask containing the reaction mixture was placed in a rotary shaking incubator at 30°C for 60 min. The reaction was stopped by adding 1:1 mixture (20 ml) of alcohol and acetone and shaken well. Phenolphthalein was used as an indicator and the liberated free fatty acids were titrated against 0.1 N NaOH [17]. The appearance of pink colour was noted as the end point.

2.3.3 Enzyme activity unit

One unit of lipase activity was defined as the amount of enzyme that releases 1 µmol fatty acid per min per ml under specified assay conditions:

$$\text{Lipase activity}(\text{U}\cdot\text{g}^{-1}) = \frac{\Delta V \times N \times 4}{V \quad (\text{Sample})} \times \frac{1{,}000}{60}$$

where $\Delta V = V_2 - V_1$, V_1 is the volume of NaOH used against the control flask, V_2 is the volume of buffer used against the experimental flask, N is the normality of NaOH, and V_{sample} is the volume of the extract; the mg conversion factor was 1,000, and the normalization factor for dilution was 60.

2.3.4 Optimization of enzyme production

The substrate concentration was optimized by taking different quantities of almond meal (5–30 g). Different mineral salt media (MC_1–MC_6) were used to provide moisture content. The composition of these moisture contents is given in Table 1. The pH value and the moisture content were

Table 1: Comparative evaluation of different moisture contents for superior lipase activity*

Moisture content	Composition ($g \cdot l^{-1}$)	pH	Lipase activity ($U \cdot g^{-1}$)		Carbon source	Organism	Fermentation technique	Bibliography
			Literature	Present work				
MC.1	$(NH_4)_2SO_4$ 3.0, Na_2SO_4 3.2, K_2HPO_4 0.05, $MgSO_4$ 0.5, $Ca(NO_3)_2$ 0.01	7.0	10.49	10.42 ± 0.09	—	Extreme acidophilic microbes	Submerged fermentation	[18]
MC.2	K_2HPO_4 1.8, NH_4Cl 4.0, $MgSO_4$ 0.2, NaCl 0.1, $FeSO_4$ 0.01	6.9	1.82	6.69 ± 0.36	Crude oil	Wastewater bacteria	Submerged fermentation	[19]
MC.3	$MgSO_4$ 0.2, $CaCl_2$ 0.02, KH_2PO_4 1.0, K_2HPO_4 1.0, NH_4NO_3 1.0	7.2	2.40	8.53 ± 0.13	Oil	Aerobic soil bacteria	Submerged fermentation	[20]
MC.4	K_2HPO_4 1.73, KH_2PO_4 0.68, $MgSO_4$ 0.1, NaCl 4.0, $FeSO_4$ 0.03, NH_4NO_3 1.0, $CaCl_2$ 0.02, $C_6H_{12}O_6$ 5.0	7.0	4.76	7.51 ± 0.24	Glucose	*Staphylococcus lentus*	Submerged fermentation	[21]
MC.5	$NaNO_3$ 2.0, NaCl 0.8, KCl 0.8, $CaCl_2$ 0.1, KH_2PO_4 2.0, Na_2HPO_4 2.0, $MgSO_4$ 0.2, $FeSO_4$ 0.001	6.8	1.73	4.67 ± 0.16	Crude oil	*Bacillus* sp.	Submerged fermentation	[22]
MC.6	KCl 0.05, KH_2PO_4 0.1, $MgSO_4$ 0.05, K_2CO_3 0.3	7.8	1.26	6.28 ± 0.08	Sucrose	*Phytophthora parasitica*	Submerged fermentation	[23]

*Almond meal, 15 g; moisture content, 10 ml; time of incubation, 72 h; and size of inoculum, 1 ml (5%, v/w).
± Indicate standard deviation (sd) among the values of three parallel replicates. The sum-mean values differ significantly at $\rho \leq 0.05$ from each other using one-way ANOVA (LSD~5.05, Duncan's value: 10.48).

adjusted. The time of incubation and size of inoculum were also optimized.

2.3.5 Analysis of lipase-catalysed culture broth via GC/MS

The fatty acids being synthesized by fungal lipase under optimal batch conditions were analysed on an Agilent gas chromatograph (GC, AgiTech-7260) and mass spectrometer (MS, Maspec-6595) following the described method [24]. All runs were accomplished using a 20 m × 0.3 mm (as internal diameter) fused-silica capillary column with a 0.45 µm coated 6% phenylmethyl silicone film. Degassing was carried out at 180°C for 2 h, and the adsorption–desorption isotherms were recorded at 64 and 236 K under a nitrogen flow. He (99.99% purity) was used as a carrier gas. The injector temperature was adjusted to 250°C. The temperature of the ion source was set at 220°C. The ionization mode remained electron-impacted at an electron energy of 75 eV. Heptadecanoic acid methyl ester (C18:0) was selected as the sole standard material.

2.3.6 Preparation of *Mentha spicata* leaf extracts

Fresh leaves of *M. spicata* were collected from the Department of Botany of GCU Lahore, and these were washed with distilled water and dried in an oven at 40°C for 24 h. The leaves were ground, and their extract was prepared by suspending 10 g of the powder in 50 ml of ethanol at 120 rpm (30°C) for 1 h. The suspension was placed in a centrifuge machine (3K30 SIGMA laboratory centrifuges, USA) at 4,500 × *g* for 15 min [25]. The concentration of dried leaf powder of *M. spicata* was compared with different ethanol concentrations (2.5–15 ml) at different temperatures (20–50°C) for optimization of the extract preparation.

2.3.7 Green synthesis of Al-NPs

The NPs were synthesized using 100 ml of 1 mM $Al(NO_3)_3$ solution. This solution was stirred at room temperature for 10 min and 10 ml of *M. spicata* leaf extract was added slowly at room temperature. The pH of the reaction mixture was adjusted to 11 by drop-wise addition of 1 M NaOH. The change in the colour of the reaction mixture was recorded at 65°C for 30 min. The colour of the reaction mixture was changed from transparent (before the addition of leaf extract) to light yellow (after the addition of leaf extract) and then to dark yellow (after adjusting the pH

and heating at 65°C for 30 min). This change in the colour of the reaction mixture indicated the synthesis of Al_2O_3 NPs. The obtained NPs were centrifuged at 6,000 × *g* for 20 min to pelletize the NPs, which were then dried overnight at 37°C, as shown in Figure 1(b) [26].

2.3.8 Characterization of Al-NPs

Different techniques were used for the characterization of green-synthesized Al-NPs.

2.3.9 UV-visible digital spectrophotometry

The surface plasmon resonance of Al-NPs present in isopropanol was analysed using a UV-Visible Digital spectrophotometer (Cary 60, Agilent Technology, USA) at the Department of Chemistry, GC University, Lahore [27].

2.3.10 Fourier transform infrared spectroscopy

The functional groups that were responsible for the stabilization of Al-NPs were detected using a Fourier transform infrared spectroscope (IRPrestige-21, Shimadzu, Japan) at the Center for Applied Studies of Physics (CASP), GC University, Lahore [28].

2.3.11 X-ray diffraction analysis

The crystalline nature of green-synthesized NPs was confirmed using an X-ray diffractometer. The PAN Analytical X'Pert Powder XRD facility at the Lahore College Women's University was used for this purpose [29].

2.3.12 Scanning electron microscopy

The morphology and size distribution of Al-NPs were determined using a scanning electron microscope (JSM-6480LV, Jeol, Japan)at the CASP, GC University, Lahore [30].

2.3.13 Resolution of (R,S)-2-octanol by immobilized lipase-Al-NPs

The immobilized lipase (20 $U{\cdot}g^{-1}$) on Al_2O_3 NPs was dispersed in 10 ml of *n*-hexane containing racemic 2-octanol (1 mmol), acetyl chloride (2 mmol), and water (activity 0.56). The reaction vials were shaken at 160 rpm at 50°C, and the samples were withdrawn periodically for analysis using a UV/Vis spectrophotometer [31]. All the reaction parameters, such as the enzyme volume (2.5–15 µl), *n*-hexane volume (1.5–4.5 ml), 2-octanol concentration (0.25–1%), and agitation intensity (120-240 rpm) were estimated for improved resolution.

2.3.14 Statistical analysis

Treatment effects were compared by post-hoc and protected least significant difference method using one-way ANOVA (Spss-20) [32]. Significance differences among the three parallel replicates are presented as Duncan's multiple ranges in probability (<ρ>) values.

3 Results and discussion

3.1 Optimization for lipase production

Enzyme production from microbial sources is significantly dependent on the nature and concentration of the substrate [33]. The effect of the concentration of almond meal as a substrate on the production of lipase by *R. oligosporus* IIB-08 was studied. The enzyme activity was determined at each concentration, as shown in Figure 2a. As the substrate concentration increased gradually, an increase in enzyme activity was observed. The highest enzyme activity of 9.44 ± 0.06 $U{\cdot}g^{-1}$ was achieved at 15 g of almond meal, and then it decreased. In a similar study, the authors used almond meal as a substrate and reported high lipase activity (48 $U{\cdot}g^{-1}$) [8]. Fungi are highly adaptable to grow and produce enzymes under low moisture conditions [34]. The influence of different moisture contents on the formation of lipase by *R. oligosporus* IIB-08 was estimated. The different moisture contents, including distilled water, are compared in Table 1. The lipase activity for moisture contents is shown in Figure 2b. The highest enzyme activity of 10.42 ± 0.09 $U{\cdot}g^{-1}$ was observed by MC.1. The lipase activity of MC.1 was 9.2%, which is greater than the lipase activity of distilled water (9.46 ± 0.11 $U{\cdot}g^{-1}$). This indicates that MC.1 contained suitable mineral salts and humidity, which increased the production of lipase. However, in another study, distilled water was shown to have a positive effect on lipase activity at a concentration of 70% [2].

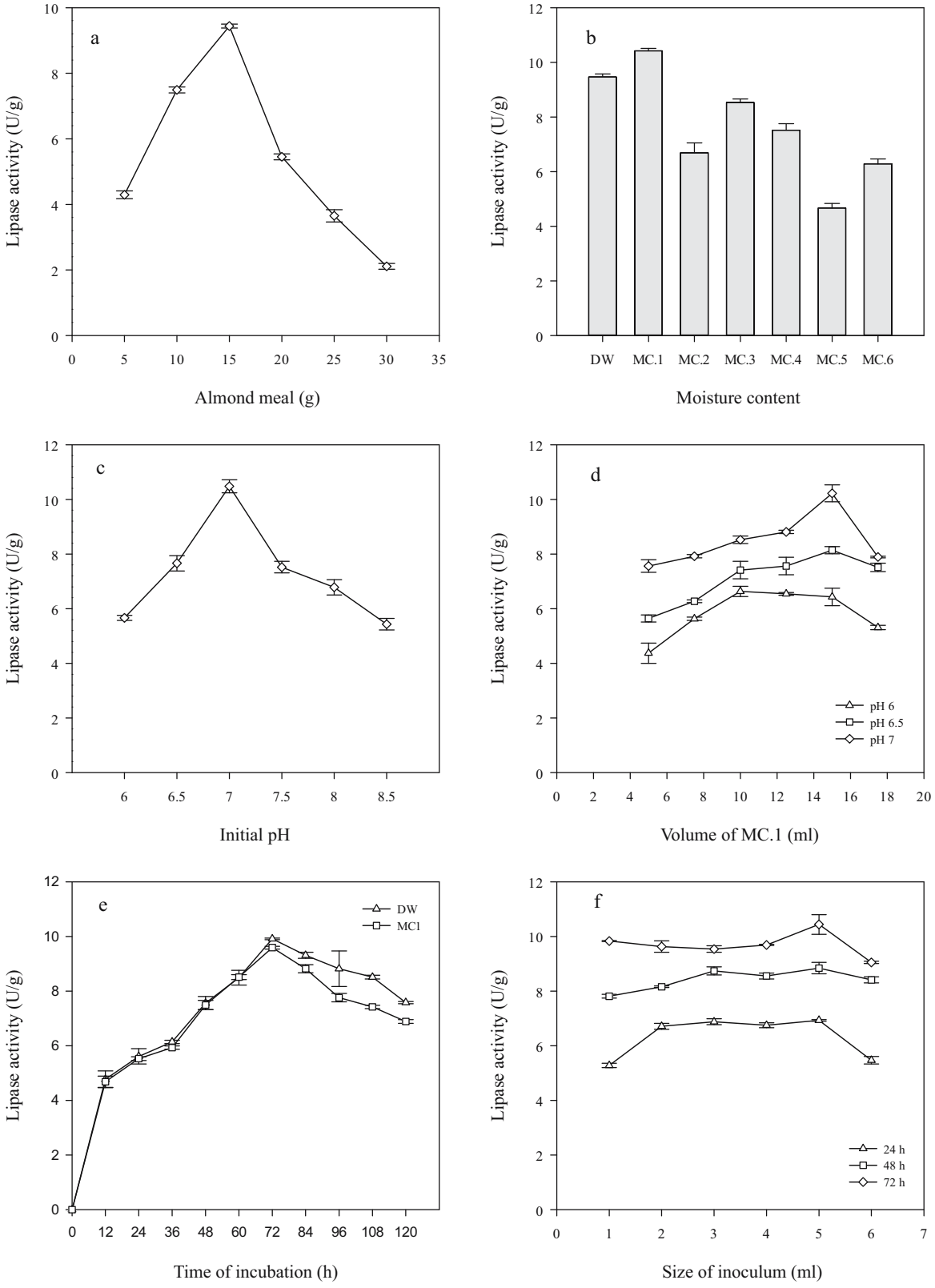

Figure 2: Optimization of lipase production by *R. oligosporus* IIB-08: (a) almond meal, (b) moisture content, (c) pH, (d) volume, (e) incubation time, and (f) size of inoculum. Almond meal, 15 g; moisture content, 15 ml; distilled water; initial pH, 7; time of incubation, 72 h; and size of inoculum, 5 ml. The error bars indicate standard deviation (±sd) among the values of three parallel replicates. The sum-mean values differ significantly at $p \leq 0.05$ from each other in one set, using one-way ANOVA (LSD~1.38, Duncan's value 10.44).

Lipase production is highly controlled by the initial pH of the growth medium [35]. The effect of different pH values of MC.1 on the production of lipase by *R. oligosporus* IIB-08 was determined. The different initial pH values of MC.1 were compared and lipase activity was measured, as shown in Figure 2c. The maximum enzyme activity in the range of 10.48 ± 0.24 $U{\cdot}g^{-1}$ was observed at pH 7 of MC.1. The improved enzyme activity near neutral pH indicated that both fungal growth and lipase production were enhanced. Other authors studied the properties of lipases, and it was found that usually, these enzymes remain stable under neutral pH [36]. The suitable concentration of moisture is the crucial requirement during solid-substrate fermentation [37]. The influence of different volumes of MC.1 on the formation of lipase by *R. oligosporus* IIB-08 was assessed. The lipase activity was determined at each volume of MC.1, as shown in Figure 2d. At initial pH of 6 and 6.5, the increase in the volume of MC.1 was a 1.5- and 1.4-fold increase in enzyme activity, respectively. At initial pH 7, the highest enzyme activity of 10.22 ± 0.31 $U{\cdot}g^{-1}$ was observed at 15 ml of MC.1. The improved enzyme activity may be due to the presence of good moisture content. Other researchers reported that 75% (v/w) moisture content was found best for the optimum production of lipases from *Aspergillus niger* [34].

Different incubation times were evaluated for lipase production. The lipase activity was determined at each time interval, as shown in Figure 2e. At 12 h, the growth of microorganisms was in the log phase. As the time was increased, the lipase activity at both moisture contents increased due to the exponential growth. The highest lipase activity of 9.91 ± 0.03 $U{\cdot}g^{-1}$ was recorded at a 72 h incubation period for distilled water. After 72 h, the increase in the incubation period decreased gradually in lipase activity. In a declining growth phase, the production of certain toxins in the growth medium resulted in the death of the microorganism. The optimization of the size of the inoculum for improved fungal growth and lipase production is essential [37]. The different sizes of inoculum were compared at three different incubation periods, as shown in Figure 2f. At 24 h incubation period, the increase in the size of the inoculum resulted in an increase in the enzyme activity up to 6.93 ± 0.03 $U{\cdot}g^{-1}$. At 48 h incubation period, the increase in the size of the inoculum resulted in an increased enzyme activity up to 1.13-fold. The highest lipase activity recorded at 72 h time interval with 5 ml inoculum size was 10.44 ± 0.36 $U{\cdot}g^{-1}$. The statistical analysis performed in triplicates showed that LSD and Duncan's values were 1.38 and 10.44, respectively. The researchers reported different conditions to produce lipase from *R. oligosporus* GCBR-3 and found that 1% inoculum size to be highly suitable for increased enzyme production [8].

3.2 Analysis of lipase-catalysed culture broth using Agilent GC/MS

Lipase-catalysed fatty acids, *viz.* linolenic acid (C18:3), linoleic acid (C18:2), palmitic acid (C16:0), and oleic acid (C18:1), detected in the culture broth via GC/MS. The results are shown in Table 2 and Figure 3. Among the fatty acids, the highest concentration of 142 $\mu g{\cdot}ml^{-1}$ with a retention time of 23.2 min was confirmed for palmitic acid. A better lipid conversion occurred, probably due to higher catalytic deficiency of the fungal lipase. This also indicated the stability of the enzyme towards its substrate catalysis. The amine groups improved the electrostatic interactions due to the negative charge decreasing the substrate surface as well as decreasing the steric hindrance of the enzyme [24].

Table 2: GC/MS analysis of different fatty acids being synthesized by fungal lipase under optimal batch conditions*

Fatty acids	Major class	Chemical structure	Retention time (min)	Confirmation ions (*m/z*)	Concentration ($\mu g{\cdot}ml^{-1}$)
Linolenic acid	C18:3	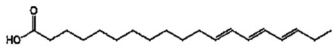	7.5	58.15	18
Linoleic acid	C18:2	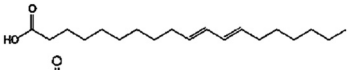	16.4	147.64	129
Palmitic acid	C16:0	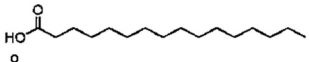	23.2	368.28	142
Oleic acid	C18:1	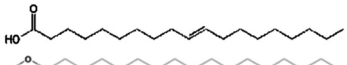	27.5	625.51	85
Heptadecanoic acid methyl ester	C18:0	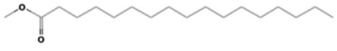	21.4	346.16	—

*Initial temperature, 55°C; initial time, 3 min; temperature increasing rate, 8°C·min^{-1} up to 160°C and 5°C·min^{-1} to 210°C while the final temperature was 210°C for 10 min.

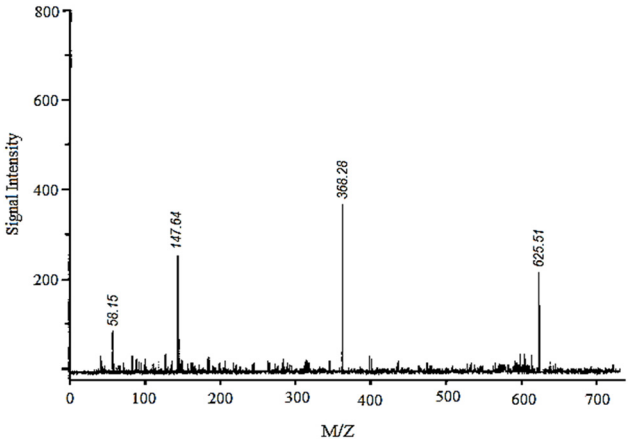

Figure 3: Analysis of lipase-catalysed culture broth via GC/MS.

Therefore, enzyme degradation is less likely to occur during application and subsequently leads to higher productivity of the catalysed products. In addition, it was also hypothesized that the use of almond meal as a basal substrate might have facilitated the formation of an active complex between enzyme's active sites and substrate by creating a larger polar area.

3.3 Optimization for the preparation of leaf extracts

The preparation of leaf extracts containing the best concentrations of active reducing species is very important. Therefore, the effect of concentration of leaf powder for the preparation of *Mentha spicata* leaf extract was studied. Different concentrations of the leaf powder were compared, and absorbance was recorded at 545 nm at each concentration, as shown in Figure 4a. The best absorbance of the leaf extract was observed at 1.5 g of leaf powder. This indicates that 1.5 g of powder was optimum for the preparation of the leaf extract. At this concentration, the absorbance was 1.01. As the concentration of leaf powder was increased from 1.5 g, a gradual decrease in the absorbance value was recorded. The very low absorbance of 0.42 was measured at 3 g of leaf powder. The optimal absorbance value of the leaf extract at 1.5 g leaf powder was 58.4% higher than the lowest value. The decline in absorbance could be due to decreased polyphenolic compounds in the leaf extract.

The determination of suitable solvent concentration plays an important role in the preparation of leaf extract. The effect of ethanol concentration and different concentrations of leaf powder in the preparation of *M. spicata* leaf extract was also studied. The absorbance at each

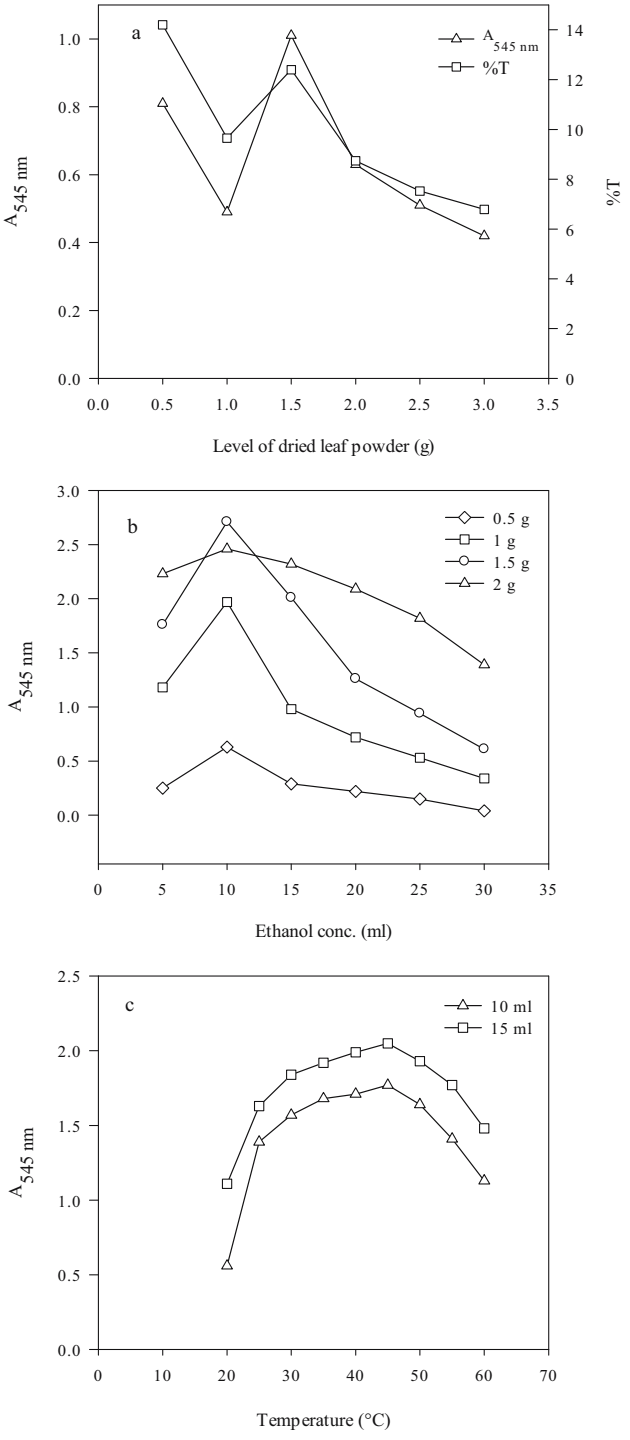

Figure 4: Optimization for the preparation of *M. spicata* leaf extract: (a) leaf powder, (b) ethanol concentration, and (c) temperature. Leaf powder, 1.5 g; ethanol, 10 ml; and temperature, 30°C.

concentration was recorded at 545 nm, as shown in Figure 4b. At 5 ml of ethanol, the best absorbance of ethanol was observed with 2 g of leaf powder. As the concentration of ethanol was increased to 10 ml, the maximum absorbance

was observed at 1.5 g of leaf powder. A gradual decrease in the absorbance value was observed at 15–30 ml of ethanol at all four concentrations of leaf powder. The lower absorbance could be due to the dilution of leaf extract at a higher volume of ethanol. Kapp et al. have found the highest content of polyphenols, up to 61.4%, in *Mentha piperata* leaf extracts [38].

The selection of extraction temperature and drying procedure are very efficient parameters for obtaining reducing compounds from leaves. The effect of different extraction temperatures on the absorbance of *M. spicata* leaf extract was studied. The absorbance was recorded at 545 nm, as shown in Figure 4c. At 20°C, absorbances of 0.56 and 1.11 were observed at 10 and 15 ml of ethanol, respectively. As the temperature was increased from this point, absorbance values increased gradually at both concentrations of ethanol. The highest absorbance detected at 45°C with 15 ml ethanol was 2.05. At 45°C, the kinetic energy of the solvent molecules was best for extracting active compounds from the leaf powder. After 45°C, a decrease in absorbance value was observed. The increase in the extraction temperature could only increase the absorbance up to a definite temperature. However, it has been reported in the literature that 100°C is the best temperature for the preparation of leaf extract [39].

3.4 Characterization of Al-NPs

UV-visible spectrophotometer is a very convenient and reliable tool for the basic categorization of Al-NPs [27]. This instrument was used to monitor the synthesis and stability of Al-NPs. The characterization of NPs was performed by using a UV-visible spectrophotometer (Cary 60, version 2). The homogeneous NP solutions were analysed at different wavelengths (200–800 nm), as shown in Figure 5(a) and (b). The UV-Vis scan rate was 24,000 nm with a dual beam. The average scanning time of the UV-Vis beam was 0.0125 s. The absorbance peak for aq. Al-NPs dispersed in deionized water was observed at 672 nm. This peak was not in coherence with the literature and it showed the presence of minute impurities along with Al-NPs. However, the absorbance peak for aq. Al-NPs suspended in isopropanol was observed at 360 nm. The highest absorbance peak for Al-NPs by other authors was also observed at 380 nm and it confirmed the formation of Al-NPs [40].

FTIR analysis was performed to detect the presence of different stabilizing functional groups adsorbed on the crystal surface of Al_2O_3 NPs. The FTIR spectra of both types

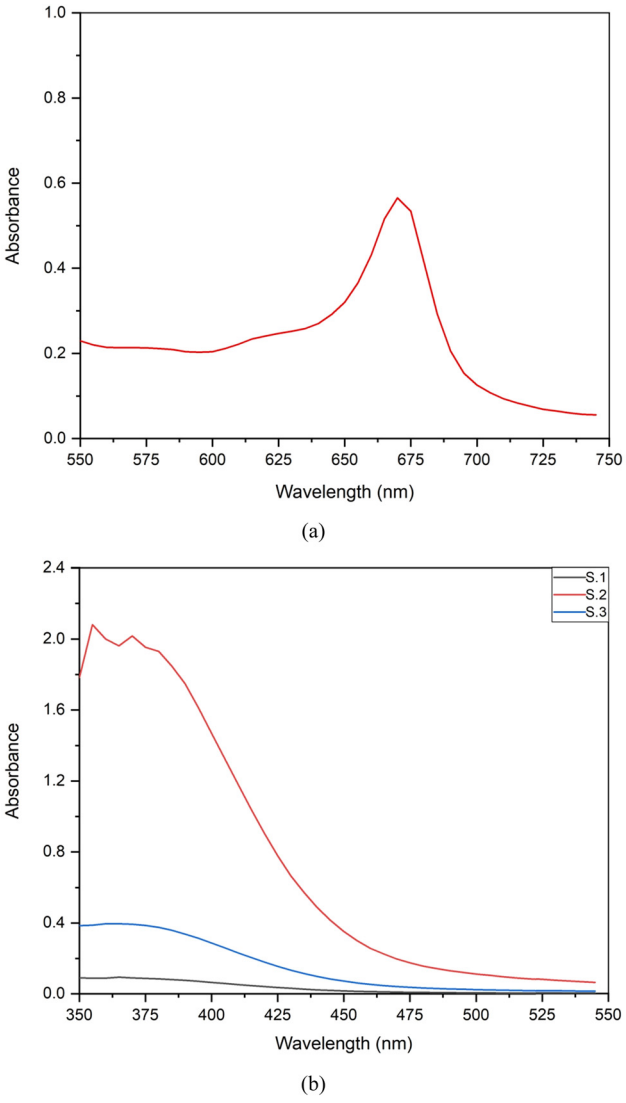

Figure 5: UV-visible absorption spectrum of Al-NPs synthesized biogenically using *M. spicata* extracts: (a) aq. Al-NPs dispersed in distilled water and (b) aq. Al-NPs dispersed in isopropanol (sample 1, sample 2, and sample 3).

of Al-NPs were recorded at the wave number range of 400–4,000/cm. The results of the FTIR analysis of both Eth-Al-NPs and Aq. Al-NPs are shown in Figure 6. In the FTIR spectrum of Eth-Al-NPs, a strong absorption band was observed at 3,344.5/cm due to the stretching vibration of the hydroxyl group (O–H) and confirmed the presence of water molecules on these NPs. The absorption values of 2,927.9 and 2,845.1/cm were caused by the C–H and N–H functional groups, respectively. The absorption bands at 1,589.3 and 1,259.5/cm were due to C═O and C–C bonds, respectively. The bending vibration of C–O was detected at 1,002.9/cm. The Al–O stretch was observed at 653.8/cm, with the strongest absorption band, in the FTIR spectrum of aq.

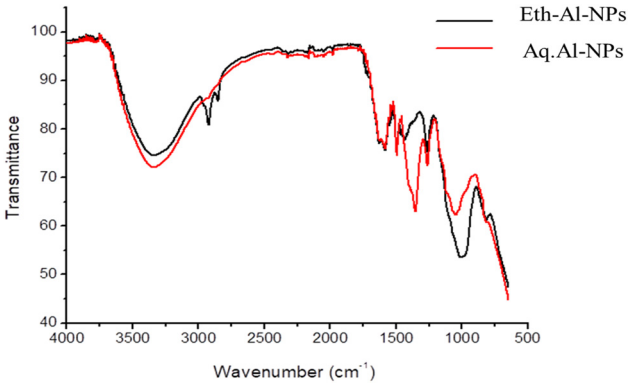

Figure 6: FTIR spectra of Al-NPs synthesized biogenically using *M. spicata* extracts.

Al-NPs, a strong absorption band at 3,340.7/cm confirmed the presence of hydroxyl functional groups. The absorption bands at 2,912.5 and 2,324.2/cm were due to C–H and N–H functional groups. The absorption values of 1,597.7 and 1,357.8/cm were observed due to the C=O and C–C functional groups, respectively. The vibration of the C–O functional group was detected in an absorption band at 1,041.5/cm. The Al–O stretch was represented by the absorption band present at 661.2/cm.

In this study, the crystalline nature of the biologically synthesized Al_2O_3 NPs was confirmed by X-ray diffractometer. The instrument was operated by continuous scanning in a wide range of angles. The scanning step was 0.02°/s, and the time taken for one step was 0.2 s. The instrument equipped with a copper anode having a K_α wavelength of 0.1540598 nm was used. The XRD profiles of aq. Al-NPs are shown in Figure 7. The peaks were indexed by using Powder X software. The peaks were found to be in correspondence

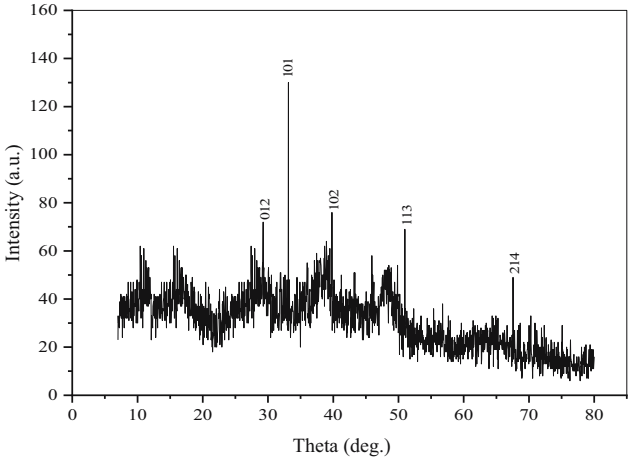

Figure 7: X-ray diffraction pattern of aq. Al-NPs synthesized biogenically using *M. spicata* extracts.

with the record of aluminium oxide structure(JCPDS card number 42-1468). The peaks were detected at different angles, *viz.* 29.24°, 33.12°, 39.8°, 50.96°, and 67.56°. The Miller indices of these peaks were 012, 101, 102, 113, and 214, respectively, in accordance with the literature. All these findings confirmed the formation of Al-NPs along with the small proportion of aluminium hydroxide. Other researchers also reported similar peaks of Al_2O_3 NPs in the XRD profile [27]. The highest crystallographic plane was found at a Miller index of 110.

In the current study, SEM was used to evaluate the size and shape of the biosynthesized Al_2O_3 NPs. The sample was observed at an accelerating voltage of 20 kV. The SEM micrographs of aq. Al-NPs, which were resolved at different magnifications, i.e. 50, 5, and 1 µm, are shown in Figure 8. The surface and morphology of the NPs were analysed. The presence of spherical-shaped Al-NPs was confirmed. The particle size of these NPs was found to be between 130 and 135 nm at a magnification of 1 µm. In a similar study, the authors also reported the green synthesis of Al-NPs and studied their bactericidal potential [27]. The authors reported the size of NPs to be 34.5 nm.

3.5 Effective resolution of 2-octanol using biogenic Al_2O_3 nanocoupled fungal lipase

The rate of a reaction catalysed by an enzyme depends upon its concentration. Therefore, the effect of different enzyme concentrations on the resolution of 2-octanol by lipase immobilized on biogenically synthesized Al_2O_3-NPs was evaluated. Two different types of enzymes, e.g. filtered and centrifuged, were compared at different concentrations. The absorbance value was recorded at each enzyme concentration, as shown in Figure 9. The experiment was carried out by using two types of Al_2O_3-NPs. At 2.5 µl of the enzyme, the best resolution of 2-octanol was obtained with the conjugate of filtered enzyme and ethanolic Al_2O_3-NPs. After 2.5 µl, the increase in the concentration of enzyme improved the resolution. The superior resolution was obtained at 12.5 µl of the enzyme with the conjugate of filtered enzyme and ethanolic Al_2O_3-NPs. The absorbance at this point was 1.57. The low resolution at higher concentrations indicated that the microenvironment or conformation of the enzyme was disturbed in the reaction system. It has been reported that the resolution of 2-octanol was improved in the reaction mixture by varying the concentrations of immobilized enzymes [31].

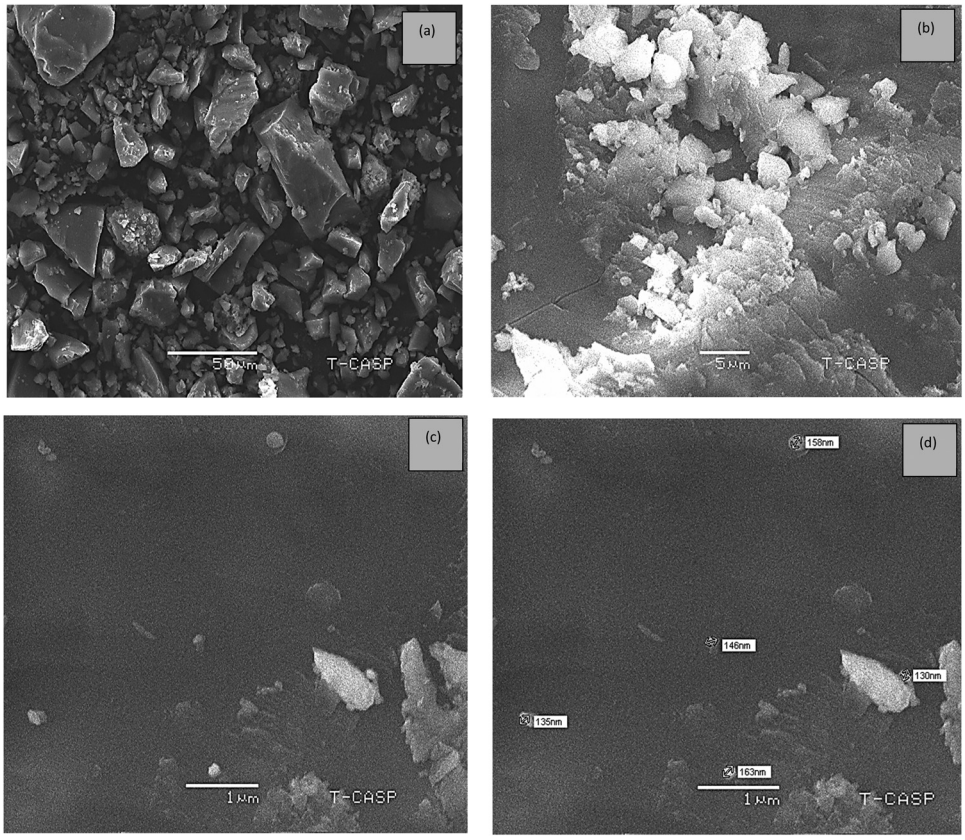

Figure 8: SEM micrographs of Al-NPs resolved at different magnifications (a) at 50 µm, (b) at 5 µm, and (c) and (d) at 1 µm.

The study of the effect of different concentrations of *n*-hexane on the resolution of 2-octanol is shown in Figure 10. Different concentrations s of *n*-hexane were compared with both types of Al_2O_3-NPs. At 0.5 ml of *n*-hexane, a good resolution was achieved from lipase immobilized on aq. Al_2O_3-NPs. As the concentration of *n*-hexane was increased gradually, a prominent increase in the resolution was observed. The best resolution was recorded at 2.5 ml of *n*-hexane with the conjugate of lipase and aq. Al_2O_3-NPs. After 2.5 ml of ethanol, the resolution level decreased by increasing the concentration of *n*-hexane. Other researchers compared *n*-heptane, acetonitrile, and toluene as organic solvents on the resolution reaction and reported highest *E*-value (71.5 ± 2.2) and enzyme activity (0.19 ± 0.01) with *n*-hexane [41].

The concentration of 2-octanol as a substrate has a great influence on enzyme reactions [41]. The estimation of the effect of concentration of 2-octanol on its resolution is shown in Figure 11. Different concentrations of 2-octanol were evaluated. Two differently produced Al_2O_3-NPs, i.e. Eth-NPs and aq. NPs were conjugated with lipase. At 0.25 ml 2-octanol, the resolution was observed with both Eth-Al_2O_3-NPs and aq. Al_2O_3-NPs. The best resolution of 2-octanol was observed at 0.5 ml with Eth-Al_2O_3-NPs. At this point, the absorbance of 0.31 was determined. After 0.5 ml of 2-octanol, the resolution was decreased by increasing the concentration. The best resolution of 2-octanol was 7.75-fold higher than the lowest point of resolution. The decreased conversion of substrate into product resulted in lower resolution. As the substrate concentration increased, the available enzyme present in the reaction mixture was reduced to catalyse the reaction. In a dissimilar study, authors reported improved enantioselectivity and enzyme activity from 41.3 to 56.8% at a substrate-to-acyl donor ratio of 2.5:1 [31].

The immobilized enzyme works efficiently only on available reactants from a bulk reaction mixture. The diffusion of reactant from the reaction mixture to the surface of the enzyme is made possible by using a suitable agitation speed [41]. The behaviour of the effect of different agitation intensities on the resolution of 2-octanol was assessed. The different agitation intensities were compared, as shown in Figure 12. Two different types of Al_2O_3-NPs were combined with lipase. The absorbance was recorded at each resolution level, which helped in the determination of the resolution of 2-octanol. In this

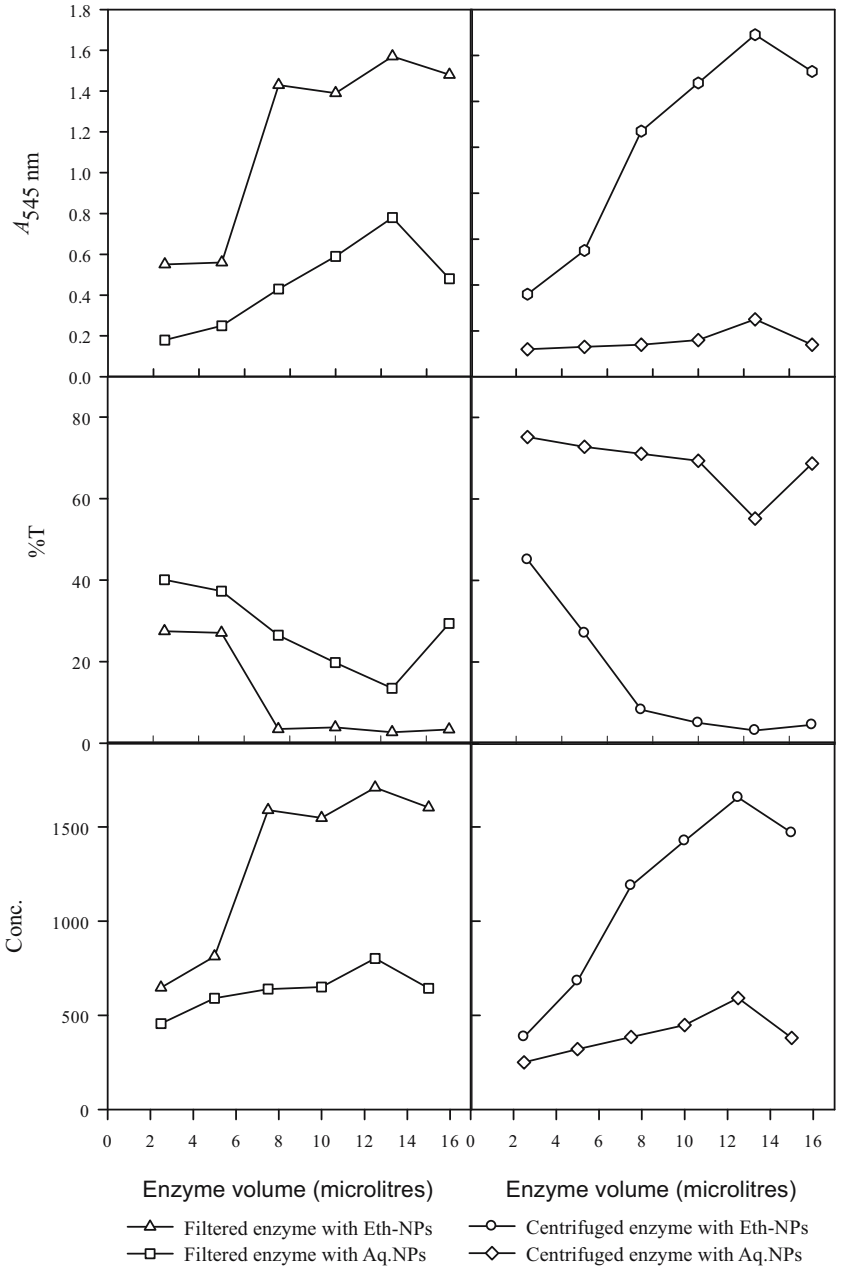

Figure 9: Effect of different enzyme volumes on resolution of 2-octanol by lipase immobilized on biogenically synthesized Al_2O_3-NPs. Almond meal, 15 g; moisture content, 15 ml; initial pH, 7; and size of inoculum, 5 ml. Leaf powder, 1.5 g; ethanol, 15 ml; and temperature, 45°C. *n*-Hexane, 3.5 ml; 2-octanol, 0.5 ml; agitation intensity, 160 rpm.

study, when an agitation intensity of 80 rpm was used, a low resolution was recorded with Eth-Al_2O_3-NPs. A gradual increase in the agitation intensity resulted in improved resolution. The superior resolution was detected at an agitation intensity of 240 rpm with aq. Al_2O_3-NPs. At this point, the absorbance value was 0.86 (at a concentration of 585). Further increase in the agitation intensity resulted in decreased resolution. At 280 rpm agitation intensity, the resolution recorded with Eth-Al_2O_3-NPs was very low. The lower resolution showed that at elevated agitation, the rate of collisions was very high, which did not allow the formation of the enzyme–substrate complex. Eventually, the product was not formed. The optimal resolution observed with aq. Al_2O_3-NPs was 2.05-fold higher than the lowest resolution value. In a similar study, the agitation speed of 200 rpm was found to be optimum for the

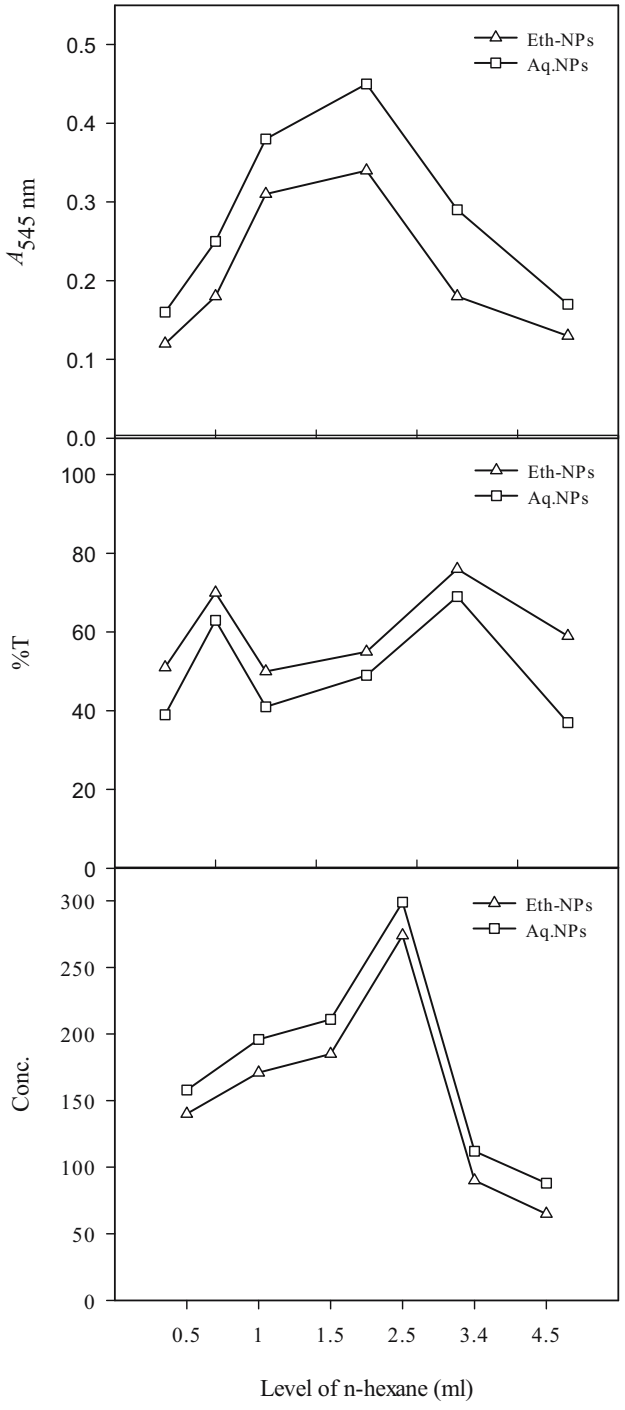

Figure 10: Effect of concentration of *n*-hexane on the resolution of 2-octanol by lipase immobilized on biogenically synthesized Al_2O_3-NPs. Almond meal, 15 g; moisture content, 15 ml; initial pH, 7; size of inoculum, 5 ml. Leaf powder, 1.5 g; ethanol, 15 ml; and temperature, 45°C. Enzyme, 12.5 µl; 2-octanol, 0.5 ml; and agitation intensity, 160 rpm.

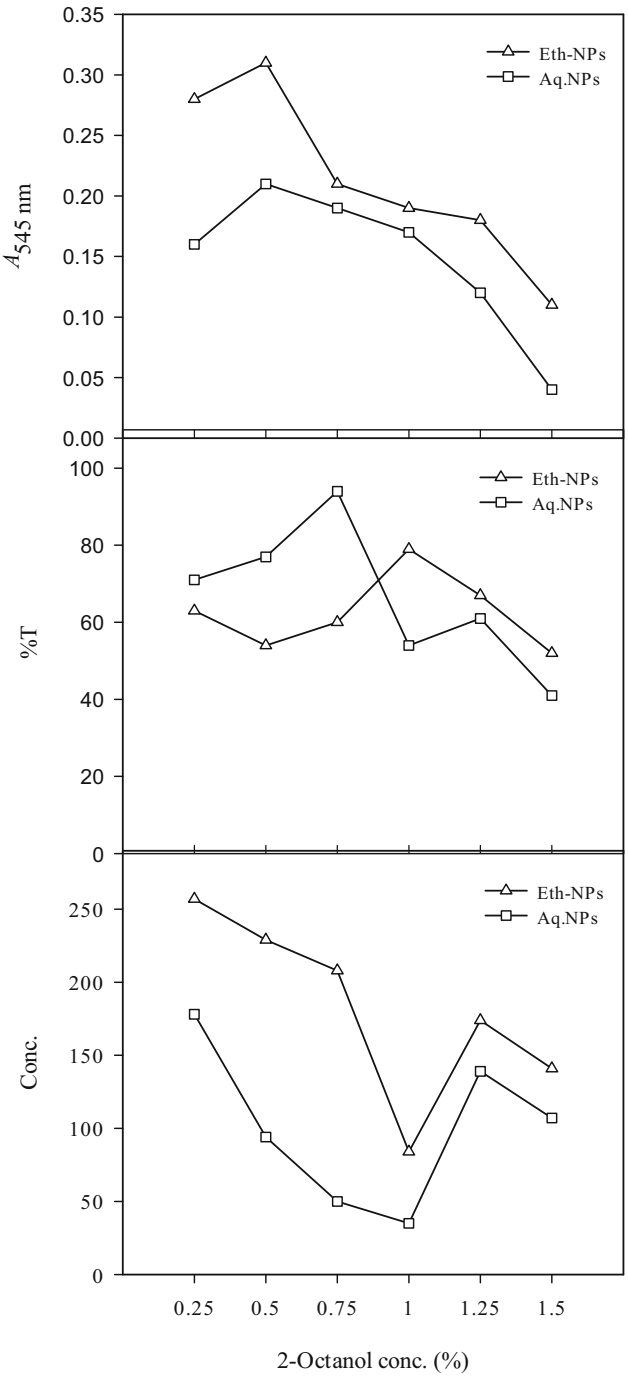

Figure 11: Effect of different 2-octanol concentration on its resolution by lipase immobilized on biogenically synthesized Al_2O_3-NPs. Almond meal, 15 g; moisture content, 15 ml; initial pH, 7; size of inoculum, 5 ml. Leaf powder, 1.5 g; ethanol, 15 ml; and temperature, 45°C. Enzyme, 12.5 µl; *n*-hexane, 2.5 ml; and agitation intensity, 160 rpm.

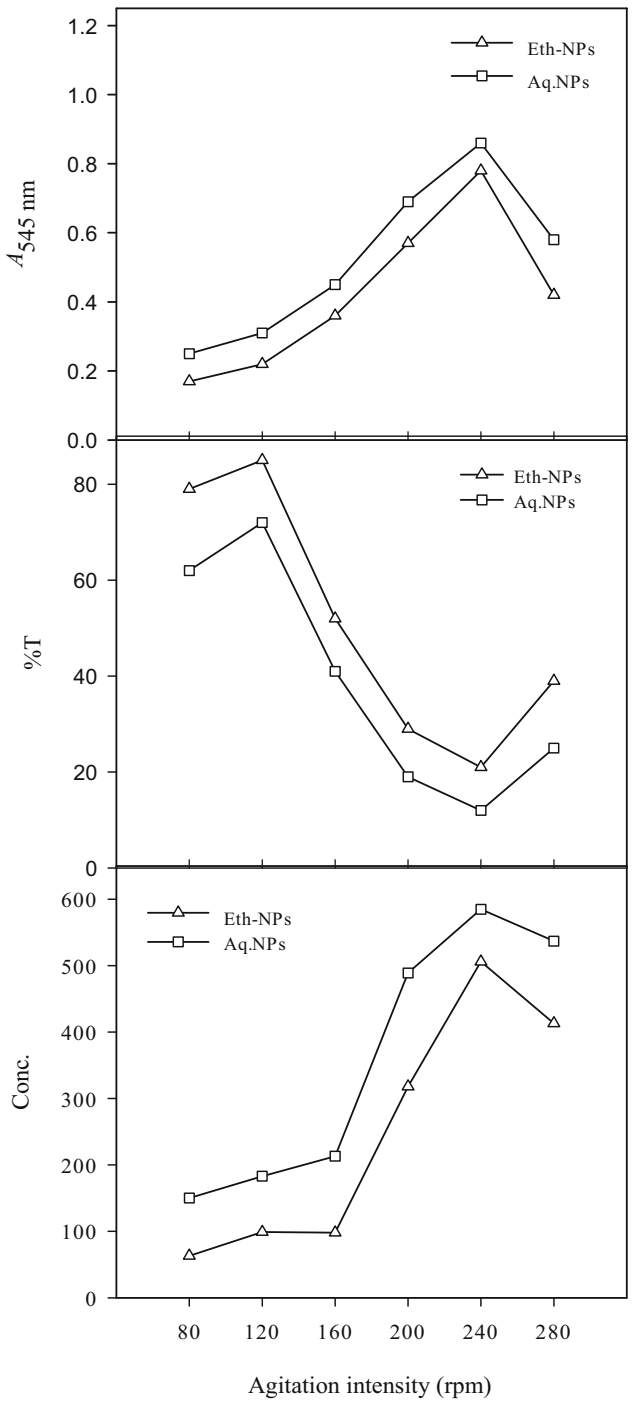

Figure 12: Effect of different agitation intensities on the resolution of 2-octanol by lipase immobilized on biogenically synthesized Al_2O_3-NPs. Almond meal, 15 g; moisture content, 15 ml; initial pH, 7; and size of inoculum, 5 ml. Leaf powder, 1.5 g; ethanol, 15 ml; and temperature, 45°C. Enzyme, 12.5 µl; *n*-hexane, 2.5 ml, and 2-octanol. 0.5 ml.

resolution of the racemic mixture [11]. However, other researchers investigated the best resolution of 2-octanol by immobilizing lipase at 160 rpm [31].

4 Conclusion

In the present study, lipase was produced from the GRAS microorganism *R. oligosporus,* and the growth conditions were optimized for obtaining improved enzyme activity. The statistical analysis performed on triplicates showed that LSD and Duncan's values were 1.38 and 10.44, respectively. The two types of Al_2O_3 NPs were prepared using the green synthesis method using *M. spicata* leaf extracts. These NPs were characterized by UV-visible spectrophotometry, FTIR spectroscopy, XRD analysis, and SEM. The enzyme and NP conjugates were found to be 9.3% effective for the resolution. As confirmed via GC/MS analysis, the better lipid conversion occurred probably due to higher catalytic deficiency of the fungal lipase. Most notably, the use of almond meal as a basal substrate facilitated the formation of an active complex between the enzyme active sites and substrate by creating a larger polar area, as indicated by the confirmation ions (346.16 *m*/*z*) of the internal standard. It was concluded that the immobilized lipases have remarkable potential to be used in the resolution of 2-octanol. However, there is a need to scale up this study for future targets.

Acknowledgements: The authors greatly acknowledge and express their gratitude to the Researchers Supporting Project (number RSPD2024R568), King Saud University, Riyadh, Saudi Arabia.

Funding information: The authors state no funding involved.

Author contributions: Conceptualization, Sikander Ali and Ghanwa Tahir; methodology, M. Usman Ahmad; software, Iram Liaqat; validation, M. Nouman Aftab; formal analysis, Shazia Khurshaid and Jahangir Khan; investigation, Abid Sarwar; resources, Tariq Aziz.; data curation, Metab Alharbi; writing – original draft preparation, Nouman Ali and M. Usman Ahmad; writing – review and editing, Tariq Aziz; visualization, Sikander Ali; supervision, Abid Sarwar and Tariq Aziz; project administration, Muhammad Abdulrahman Alashammri and Abdullah F. Alasmari.

Conflict of interest: The authors state no conflict of interest.

Data availability statement: The datasets generated during and/or analysed during the current study are available from the corresponding author on reasonable request.

References

[1] Chandra P, Enespa SR, Arora PK. Microbial lipases and their industrial applications: a comprehensive review. Microb Cell Fact. 2020;19:169. doi: 10.1186/s12934-020-01428-8.

[2] Nadeem F, Mehmood T, Anwar Z, Saeed S, Bilal M, Meer B. Optimization of bioprocess steps through response surface methodology for the production of immobilized lipase using *Chaetomium globosum* via solid-state fermentation. Biom Convers Biofin. 2021;45:124–31. doi: 10.1007/s13399-021-01752-y.

[3] Kanmani P, Kumaresan K, Aravind J, Karthikeyan S, Balan R. Enzymatic degradation of polyhydroxyalkanoate using lipase from *Bacillus subtilis*. Int J Environ Sci Technol. 2016;13:1541–52. doi: 10.1007/s13762-016-0992-5.

[4] Rajendran A, Palanisamy A, Thangavelu V. Lipase catalyzed ester synthesis for food processing industries. Braz Arch Biol Technol. 2009;52:207–19.

[5] Javed S, Azeem F, Hussain S, Rasul I, Siddique MH, Riaz M, et al. Bacterial lipases: a review on purification and characterization. Prog Biophys Mol Biol. 2018;132:23–34.

[6] Sun SY, Xu Y. Solid-state fermentation for 'whole-cell synthetic lipase' production from *Rhizopus chinensis* and identification of the functional enzyme. Proc Biochem. 2008;43:219–24.

[7] Riyadi FA, Alam MZ, Salleh MN, Salleh HM. Optimization of thermostable organic solvent-tolerant lipase production by thermotolerant *Rhizopus* sp. using solid-state fermentation of palm kernel cake. 3Biotech. 2017;7:300.

[8] Haq IU, Idrees S, Rajoka MI. Production of lipases by *Rhizopus oligosporus* by solid-state fermentation. Proc Biochem. 2002;37:637–41. doi: 10.1016/S0032-9592(01)00252-7.

[9] Khoobi M, Motevalizadeh SF, Asadgol Z, Forootanfar H, Shafiee A, Faramarzi MA. Polyethyleneimine-modified superparamagnetic Fe_3O_4 nanoparticles for lipase immobilization: characterization and application. Mat Chem Phy. 2015;149:77–86.

[10] Baker S, Rakshith D, Kavitha KS, Santosh P, Kavitha HU, Rao Y, et al. Plants: Emerging as nanofactories towards facile route in synthesis of nanoparticles. BioImpact. 2013;3:111–7.

[11] Xun E, Lv X, Kang W, Wang J, Zhang H, Wang L, et al. Immobilization of *Pseudomonas fluorescens* lipase onto magnetic nanoparticles for resolution of 2-octanol. Appl Biochem Biotechnol. 2012;168:697–707.

[12] Abdelkhaleq A, Al-Askar AA. Green synthesized ZnO nanoparticles mediated by Mentha spicata extract induce plant systemic resistance against Tobacco mosaic virus. Appl Sci. 2020;10(15):5054.

[13] Selvaraj R, Nagendran V, Varadavenkatesan T, Goveas LC, Vinayagam R. Stable silver nanoparticles synthesis using *Tabebuia aurea* leaf extract for efficient water treatment: A sustainable approach to environmental remediation. Chem Eng Res Des. 2024;208:456–63. doi: 10.1016/j.cherd.2024.07.012.

[14] Varadavenkatesan T, Nagendran V, Vinayagam R, Goveas, Selvaraj RLC. Effective degradation of dyes using silver nanoparticles synthesized from *Thunbergia grandiflora* leaf extract. Bioresour Tech Rep. 2024;27:101914. doi: 10.1016/j.biteb.2024.101914.

[15] Patel V, Shah C, Deshpande M, Madamwar D. Zinc oxide nanoparticles supported lipase immobilization for biotransformation in organic solvents: A facile synthesis of geranyl acetate, effect of operative variables and kinetic study. Appl Biochem Biotechnol. 2016;178:1630–51. doi: 10.1007/s12010-015-1972-9.

[16] Ayinla ZA, Ademakinwa AN, Agboola FK. Studies on the optimization of lipase production by *Rhizopus* sp. ZAC3 isolated from the contaminated soil of a palm oil processing shed. J Appl Biol Biotechnol. 2017;5:030–7. doi: 10.7324/JABB.2017.50205.

[17] Kundu AK, Pal N. Isolation of lipolytic fungi from soil. J Pharm Ind. 1970;32:96–7.

[18] Christel S, Dopson M. Mineral salt medium for extreme acidophilic microorganisms. Protoc Exch. 2015;44:542. doi: 10.1038/protex.2015.031.

[19] Mukred AM, Hamid AA, Hamzah A, Yusoff WMW. Growth enhancement of effective microorganisms for bioremediation of crude oil contaminated waters. Pak J Biol Sci. 2008;11:1708–12.

[20] Prabhakran P, Sureshbabu A, Rajakumar S, Ayyasamy PM. Bioremediation of crude oil in synthetic mineral salts medium enriched with aerobic bacterial consortium. Int J Innov Res Sci Eng Technol. 2014;3:9236–40.

[21] Sekar S, Mahadevan S, Kumar SSD, Mandal AB. Thermokinetic responses of metabolic activity of *Staphylococcus lentus* cultivated in glucose limited mineral salt medium. J Therm Anal Catorim. 2011;104:149–55.

[22] Sepahi AA, Golpasha ID, Emami M, Nakhoda AM. Isolation and characterization of crude oil degrading *Bacillus* sp. Iran J Environ Health Sci Eng. 2008;5:149–54.

[23] Wills WH. The utilization of carbon and nitrogen compounds by *phytophthora parasitica dastur* var. *nicotianae*. J Elisha Mitchell Sci Soc. 1954;70:231–5.

[24] Nematian T, Shakeri A, Salehi Z, Saboury AA. Lipase immobilized on functionalized superparamagnetic few-layer graphene oxide as an efficient nanobiocatalyst for biodiesel production from *Chlorella vulgaris* bio-oil. Biotechnol Biofuels. 2020;13:57. doi: 10.1186/s13068-020-01688-x.

[25] Kajani AA, Bordbar AK, Esfahani SHZ, Khosropour AR, Razmjou A. Green synthesis of silver nanoparticles with potent anticancer activity using *Taxus baccata* extract. RSC Adv. 2014;4:61394–403.

[26] Dutt A, Upadhyay LSB. Synthesis of cysteine functionalized silver nanoparticles using green tea extract with application for lipase immobilization. Anal Lett. 2018;51:1071–86. doi: 10.1080/00032719.2017.1367399.

[27] Ansari MA, Khan HM, Alzohairy MA, Jalal M, Ali SG, Pal R, et al. Green synthesis of Al_2O_3 nanoparticles and their bactericidal potential against clinical isolates of multi-drug resistant *Pseudomonas aeruginosa*. World J Microbiol Biotechnol. 2015;31:153–64. doi: 10.1007/s11274-014-1757-2.

[28] Bombalska A, Mularczyk-Oliwa M, Kwasny M, Wlodarski M, Kaliszewski M, Kopczynski K, et al. Classification of the biological material with use of FTIR spectroscopy and statistical analysis. Spectrochim Acta-A: Mol Biomol Spectrosc. 2011;78:1221–6. doi: 10.1016/j.saa.2010.10.025.

[29] Sumesh KR, Kanthavel K. Green synthesis of aluminium oxide nanoparticles and its applications in mechanical and thermal stability of hybrid natural composites. J Polym Environ. 2019;27:2189–200. doi: 10.1007/s10924-019-01506-y.

[30] Yildirim D, Baran E, Ates S, Yazici B, Tukel SS. Improvement of activity and stability of *Rhizomucor miehei* lipase by immobilization on nanoporous aluminium oxide and potassium sulfate microcrystals and their applications in the synthesis of aroma esters. Biocatal Biotransform. 2019;37:210–23. doi: 10.1080/10242422.2018.1530766.

[31] Zhao LF, Zheng LY. Resolution of 2-octanol via immobilized Pseudomonas sp. lipase in organic medium. Biocatal Biotransform. 2011;29:47–53. doi: 10.3109/102424 22.2010.551189.

[32] Snedecor GW, Cochran WG. Statistical Methods. 7th edn. Iowa, USA: Iowa State University; 1980.

[33] Burkert JFM, Maugeri F, Rodrigues MI. Optimization of extracellular lipase production by *Geotrichum sp.* using factorial design. Bioresour Technol. 2004;91:77–84.
[34] Nema A, Patnala SH, Mandari V, Kota S, Devarai SK. Production and optimization of lipase using *Aspergillus niger* MTCC 872 by solid-state fermentation. Bull Natl Res Cent. 2019;43:82. doi: 10.1186/s42269-019-0125-7.
[35] Elibol M, Ozer D. Lipase production by immobilized *Rhizopus arrhizus*. Proc Biochem. 2000;36:219–23.
[36] de Azevedo WMD, de Oliveira LFR, Alcantara MA. Cordeiro AMTM, Damasceno KSFSC, Assis CF, Junior FCS (2020) Turning cacay butter and wheat bran into substrate for lipase production by *Aspergillus terreus* NRRL-255. Prep Biochem Biotechnol. 2020;50:689–96. doi: 10.1080/10826068.2020.1728698.
[37] Iftikhar T, Niaz M, Zia MA, Haq I. Production of extracellular lipases by *Rhizopus oligosporus* in a stirred fermenter. Braz J Microbiol. 2010;41:1124–32.
[38] Kapp K, Hakala E, Orav A, Pohjala L, Vuorela P, Pussa T, et al. Commercial peppermint (*Mentha piperita* L.) teas: antichlamydial effect and polyphenolic composition. Food Res Int. 2013;53:758–66. doi: 10.1016/j.foodres. 2013.02.015.
[39] Krzyzanowska J, Janda B, Pecio L, Stochmal A, Oleszek W, Czubacka A, et al. Determination of polyphenols in Mentha longifolia and M. piperita field-grown and in vitro plant samples using UPLC-TQ-MS. J AOAC Int. 2011;94:43–50. doi: 10.1093/jaoac/94.1.43.
[40] Thanaraj S, Mitthun ANK, Geetha SP, Carmelin DS, Surya M, Saravanan M. Green synthesis of Aluminum oxide nanoparticles using Clerodendrum phlomidis and their antibacterial, anti-inflammatory, and antioxidant activities. Cureus. 2024;16(1):e52279. doi: 10.7759/cureus.52279.
[41] Sose MT, Bansode SR, Rathod VK. Solvent free lipase catalyzed synthesis of butyl caprylate. J Chem Sci. 2017;129:1755–60. doi: 10.1007/s12039-017-1391-2.